ELSEVIER

Chemical Engineering Journal 138 (2008) 608–615

Chemical Engineering Journal

www.elsevier.com/locate/cej

Effect of calcination conditions and precursor proportions on the properties of YSZ nanoparticles obtained by modified sol–gel route

C. Suciu [a,*], A.C. Hoffmann [a], A. Vik [b], F. Goga [c]

[a] *Department of Physics and Technology, University of Bergen, Allegaten 55, 5007 Bergen, Norway*
[b] *Prototech A.S., Fantoftveien 38, 5075 Bergen, Norway*
[c] *Faculty of Chemistry and Chemical Engineering, Babes-Bolyai University, 400028 Cluj-Napoca, Romania*

Received 8 May 2007; received in revised form 19 August 2007; accepted 6 September 2007

Abstract

The effect is studied of some crucial process parameters on the properties of YSZ nanoparticles produced for solid oxide fuel cell (SOFC) components by a sol–gel method using sucrose and pectin as precursors. The role of the new organic precursors in the chemical process is also discussed. The produced particles are characterized in various ways: by differential thermal analysis (DTA), by nitrogen adsorption using the BET isotherm, by X-ray diffraction (XRD), and by transmission electron microscopy (TEM). The DTA profiles of the gel are compared with those of pure sucrose in the same temperature interval, and substantial differences are seen. The XRD signature from the nanoparticles is one of cubic YSZ and no other crystalline phases. The analyses indicate a significant influence of calcination temperature on the particle size, which increases with increasing calcination temperature. The mean particle size calculated from the BET analyses, on the one hand, and the mean crystallite size from the XRD analyses calculated using the Scherrer formula, on the other, agree in terms of both order-of-magnitude and trend.

Keywords: Yttrium-stabilized zirconia; Nanoparticles; Solid oxide fuel cells; Sol–gel processing; Calcination temperature; Organic precursors

1. Introduction

The use of nanoparticles as raw materials for production of SOFC components can be advantageous in a number of respects. Finer precursor powders give rise to larger specific areas in the electrodes, and therefore a larger triple phase boundary, potentially reducing electrode polarization losses [1–3]. An electrolyte produced from nanoparticles may exhibit a finer grain structure, and thus a higher density of grain boundaries, in addition to possibly a larger crystal constant in the crystallites themselves. These are features that may increase the oxygen ion mobility and therefore the ionic conductivity, reducing ohmic losses in the cell [4,5]. Producing cell components from nanoparticles also reduces the required calcination temperature, and therefore makes cell production easier and more cost effective.

Concentrating on chemical methods used for producing zirconia-based nanoparticles, the most common are: coprecipitation with ammonia, precipitation with urea [6], citrate process [7,8], polymeric route using polyvinyl alcohol [9], sol–gel method [10], gel-combustion process [11]. All these methods present common advantages such as low costs, good control of stoichiometry, good mixing of the starting materials and good chemical homogeneity of the product. On the other hand, particle agglomeration and costly precursors are two disadvantages of this type of method. Work in this field is therefore continuing, and many new chemical methods are being developed and existing ones modified in order to improve the particles produced and the cost-effectiveness of the process [12,13].

The present authors have introduced a modified sol–gel method, using simple sucrose and pectin as organic precursors. Sucrose, made from glucose and fructose units, also known as ordinary table sugar, is probably the most abundant organic chemical in the world. Pectin is a “gum” naturally found in fruits and is mainly used as a gelling agent. A study in which a comparison was made between pure zirconium oxide particles made using conventional organic precursors, e.g. citric acid, ethylene glycol and glycerol, as opposed to particles made using sucrose and pectin was previously presented [14]. Those particles were not doped with yttrium, and the material was therefore not suitable for use in solid oxide fuel cells. The zirconium oxide

* Corresponding author.
E-mail address: crina.suciu@ift.uib.no (C. Suciu).

1385-8947/$ – see front matter © 2007 Elsevier B.V. All rights reserved.
doi:10.1016/j.cej.2007.09.020

particles obtained using sucrose and pectin had practically uniform diameters of less than 30 nm, the individual particles were clearly distinguishable, and they did not appear easily to adhere to each other. In the case of the conventional precursors, the obtained powders were largely in the form of large agglomerates, in which the individual particles were difficult to distinguish, and the particle sizes were between 50 and 60 nm.

This article focuses on the production of YSZ (yttrium-stabilized zirconia) particles for the production of SOFC electrolytes and anodes.

2. Objectives

While earlier research has shown that it is possible to produce yttrium-stabilized zirconia nanoparticle with a cubic crystal structure with the sol–gel process using the new organic precursors, the objective of the present work was to:

(1) study the effects of two important process parameters: the calcination temperature and the pectin/sucrose ratio on the quality of the produced particles;
(2) identify approximate optimal values for these parameters, and, as a corollary:
(3) determine the tolerance of the process to variations in these process parameters.

A further objective was to gain some preliminary insight into the probable role played by the organic precursors in the process.

3. Experimental work

Zirconium tetrachloride ($ZrCl_4$, Sigma–Aldrich, technical purity) and yttrium nitrate hexahydrate ($Y(NO_3)_3{\cdot}6H_2O$, Sigma–Aldrich, 99.9% purity) were adopted as starting materials. The appropriate quantities for a final composition of 8 mol% Y_2O_3 to ZrO_2 were calculated and used. Commercial sucrose and pectin were used for gel preparation in the sucrose:pectin mass ratios shown in Table 1. To create these proportions the amount of sucrose was kept constant and only the amount of pectin was varied.

One more sample, called Z, was created containing only the organic precursors. This sample was subjected to thermal analysis (see below) for comparison with the samples A, B, and C.

The method involves mixing together two water-based solutions, one containing the Zr and Y salts and another one containing the sucrose:pectin mixture. These two solutions are homogenized together on a warming plate by adding the sucrose:pectin solution drop wise to the salts solution under continuous stirring. The clear, homogeneous solutions obtained

Table 1
The sucrose:pectin mass ratios used

	A	B	C
Sucrose	100	100	100
Pectin	0.5	1.5	2.5

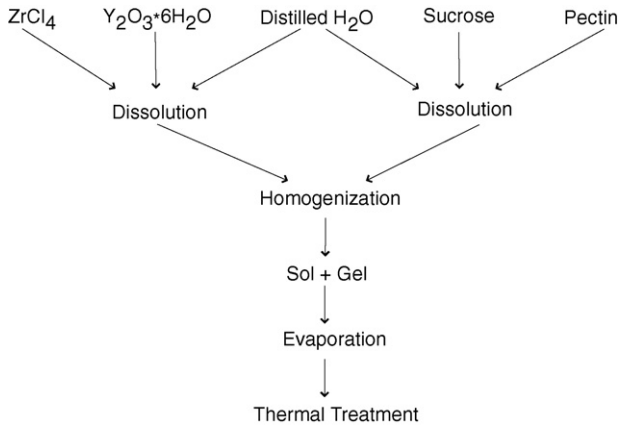

Fig. 1. Flow chart for the preparation of yttria-stabilized zirconia powders.

have a pH of 0.5–1. The stirring is continued for 3 h at a temperature between 90 and 110 °C. The sol and gel are gradually formed. The heating treatment continues until the whole composition becomes gellified, and in the end a xerogel is obtained. The flow chart of the method is shown in Fig. 1. Further thermal treatment, at temperatures of 500, 700, 900 and 1000 °C, will transform the xerogel, into cubic YSZ as the results show.

The calcination treatment was applied in steps because of the large amount of organic compounds contained in the gel. The temperature levels and durations of these steps were planned in the light of the results of the TA analysis (see below) to allow the processes, such as dewatering, to go to completion before proceeding with raising the temperature. The calcination treatment applied to the samples at 500, 700, 900 and 1000 °C were as follows: the heating or cooling rates were always 100 °C per hour, and the temperature held constant at certain plateaus, the level of each was inferred by the thermal analysis described in a later section, to allow completion of each of the processes taking place at that temperature before continuing heating. The plateaus were as follows:

- 500 °C: 1 h at 200 °C, 2 h at 400 °C and 6 h at 500 °C;
- 700 °C: 1 h at 200 °C, 2 h at 400 °C and 4 h at 700 °C;
- 900 °C: 1 h at 200 °C, 2 h at 400 °C, 3 h at 600 °C and 3 h at 900 °C;
- 1000 °C: 1 h at 200 °C, 2 h at 400 °C, 3 h at 600 °C and 2 h at 1000 °C.

4. Results and discussion

4.1. The role of the organic precursors in the preparation route

Addition of the sucrose and pectin mixture in the solution of the metal cations form a polymer matrix in which the metal cations are distributed through the polymeric network structure. In the present research, sucrose being always in excess acts as a strong chelating agent and as a pattern material. The chelated complex mass is obtained by polymerization via gel formation and the final particles are obtained upon decomposition in the

calcination process. The sucrose molecule in aqueous solution is hydrolyzed into glucose and fructose and in this way sugar recrystallization is prevented. Afterwards, the glucose and fructose molecules are oxidized to gluconic acid or polyhydroxyl acid. Gluconic acid contains carboxylic acid group in one end and five linear hydroxyl groups which can participate in the complexation of metal ions and may form branched polymer with pectin [15–18].

The mechanism pathway can be represented as shown in the following equations:

$$C_{12}H_{22}O_{11}\,(\text{sucrose}) + H_2O \rightarrow C_6H_{12}O_6\,(\text{glucose}) + C_6H_{12}O_6\,(\text{fructose}) \quad (1)$$

$$C_6H_{12}O_6(\text{fructose}) \xrightarrow{NO_3^-} C_6H_{12}O_7(\text{gluconic acid}) \xrightarrow{M^{n+}}$$

$$OH\text{–}R\text{–}C(O)(O)M^{n+}\ ;\ R = \text{-CH(OH)CH(OH)CH(OH)CH(OH)CH}_2\text{-} \quad (2)$$

$$OH\text{–}R\text{–}C(O)(O)M^{n+} + n\,HOOC\text{–}R\text{–}OH \rightarrow HO\text{-}[\text{-OC–R–O-}]_n\text{-R–}C(O)(O)M^{n+} + n\,H_2O \quad (3)$$

During heating, the metal ion complex is decomposed into CO_2 and H_2O and a large amount of heat is generated. All these products are gaseous, preventing agglomeration such that pores and fine particles with high surface area are formed in the final gel. It is well established that the degree of porosity of the gel is a direct result of the amount of gases that are released during calcination.

This ends our discussion of the role of the sucrose in the process. Below, we give an account of the structure of the pectin, and propose a possible role it might play in the process.

Pectin is a high-value functional food ingredient widely used as a gelling agent and stabilizer. Recently, there has been a tremendous progress in understanding the very complex structure of pectin polymers by the application of techniques including enzymatic fingerprinting, mass spectrometry, NMR and molecular modelling [19].

Pectin forms a family of oligosaccharides and polysaccharides that have common features, but are extremely different in their fine structures. The pectins are rich (at least 65%) in galacturonic acid (GalA) and three pectin polysaccharides are known, all containing GalA to a higher or smaller extent: homogalacturonan (HG) is a linear polymer consisting of 1,4-linked α-D-GalA; rhamnogalacturonan I (RGI) consists of the repeating disaccharide [→4)- α-D-GalA-(1→2)- α-L-Rha-(1→] with different glycan chains attached to the Rha residues; and rhamnogalacturonan II (RGII) has a backbone of HG rather than RG, with complex side chains attached to the GalA residues. Until recently it was accepted that RG and HG domains constitute the backbone of pectic polymers as shown in Fig. 2A. An alternative structure has been proposed in which HG is a long side chain of RGI (Fig. 2B). One thing that is not disputed is that pectins are an extremely complex and structurally diverse group of polymers [19].

The chain lengths of the various domains can vary considerably and a pectin gel is formed when portions of HG are cross-linked to form a three dimensional crystalline network in which water and solutes are trapped (Fig. 2C).

Pectin chains thus form some very large, long layers and sucrose molecules may bind between this layers. Thus, in the present process, metallic ions (e.g. Zr^{4+}) are bound by the

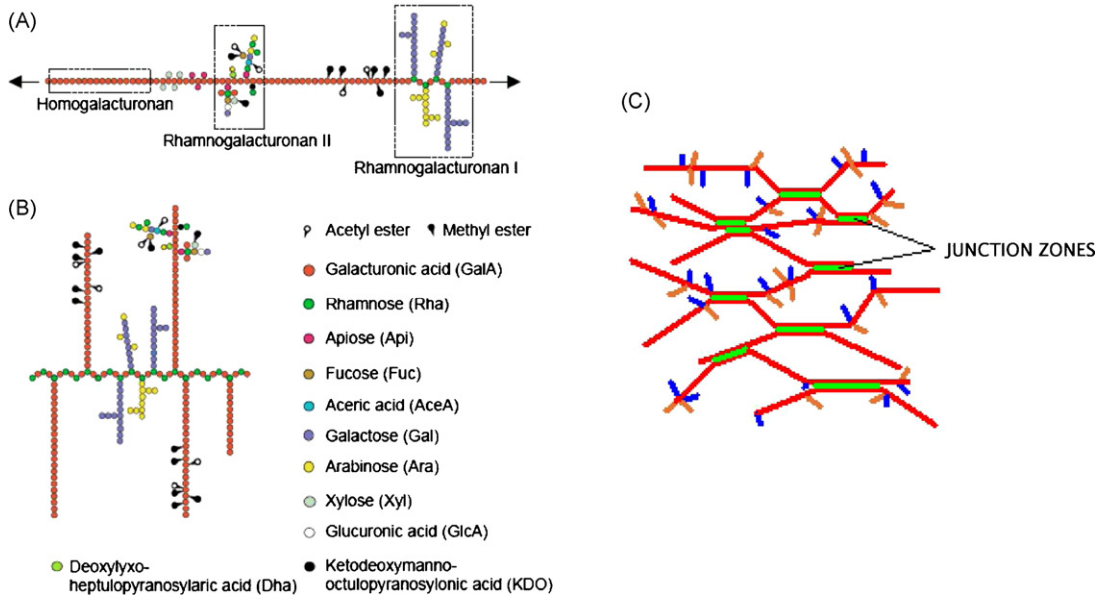

Fig. 2. (A) Schematic representations of the conventional pectin. (B) Proposed alternative structures of pectin (the polymers shown here are intended only to illustrate the major domains found in most pectins rather than definitive structures). (C) HG domains are joined at junction zones forming a crystalline network that traps water and other molecules. Figures reproduced from [19] with the authors' permission.

sucrose molecule and the resulting complex molecule is trapped between pectin layers, possibly in the junction zones).

4.2. Thermal analysis

As mentioned, the process of calcination of the dried xerogels were studied by thermal analysis (TA) using a Derivatograph Q 1500 (MOM Hungary) based on the F. Pauli, J. Pauli and L. Erdey principle. Small dried xerogel samples taken from the A, B and C samples, respectively, were analyzed at a heating rate of 10 °C/min. A sample of simple sucrose, labelled Z, was also analyzed at the same conditions for reference. The TA results are shown in Fig. 3.

For the sample Z, an endothermic process with small intensity between 180 and 200 °C can be observed. This appears to be due to the initiation of sucrose melting (the melting point of sucrose is 186 °C). Starting at 250 °C, an exothermic process takes place with an increasing intensity presenting a maximum at 500 °C. This is due to oxidation of the sucrose, also confirmed by the mass losses indicated on the TG and DTG curves. The total mass loss on the Z sample was 98%. Since the differential thermal analysis (DTA) does not present any inflections after this point, it can be assumed that all the processes are finished.

The A, B and C samples behave similarly, since the sucrose quantity remains the same in all three and only the amount of pectin content was increased to obtain proportions of 0.5–2.5 to the 100 of sucrose. Different sucrose:pectin ratios did not influence the shape of the thermal curves because the amount of sucrose was the same. The TG curve shows a process with a mass loss of 3–4% at 100 °C which takes place with low speed. This is likely due to water elimination. A strong exothermic process takes place between 280 and 300 °C and continues up to 850 °C with a slight inflection at 650 °C. These changes are due to the oxidation of the organic compounds which starts at 280 °C and continues slowly. At the same time, another exothermic process without mass variation overlaps the organics oxidation. This latter process, which starts at a low rate around 500 °C, has a point of inflection at 650 °C, a maximum at 750 °C, and continues up to 850–880 °C, is attributed to the formation of cubic ZrO_2. This interpretation is confirmed by the XRD data. At 900 °C all the processes are finished.

Sucrose in the presence of pectin, even in small amounts leads to crushable, fluffy, black powder of the oxide system. An empirical observation was that the higher the fluffiness of the powders the lower was the particle size of the final product. Due to different calcination behaviour, optimum metal ion to sucrose and pectin ratio for different powders can vary and is essential.

4.3. Specific surface area

The specific surface area was determined from nitrogen adsorption using a Gemini 2380 from Micromeritics. All the samples were degassed at 300 °C for 3 h under vacuum before analysis. The obtained BET values of the specific surface area for all the samples are shown in Table 2. The standard deviations were provided with the multipoint analyses by the data acquisition software of the instrument calculated in accordance with Gauss' error propagation formula.

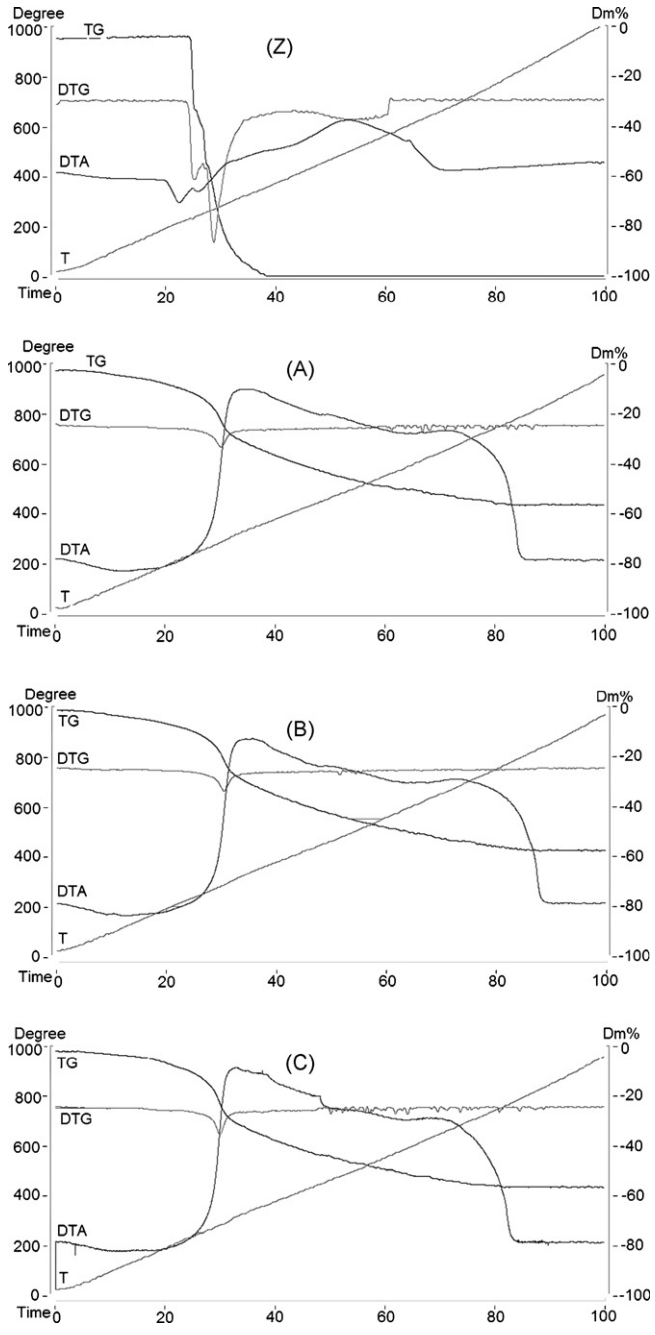

Fig. 3. The thermal analysis of the sucrose Z, A, B and C samples.

The particle size was calculated assuming that the particles are round and that the density of the cubic ZrO_2 is 5900 kg/m^3. The results are shown in Fig. 4. The data indicate that the particle size increases with increasing calcination temperature. At low temperatures the B samples, with the intermediate pectin concentration, presented the smallest particle size (11.3 and 11.71 nm at 500 °C) but at temperatures higher than 600 °C the A samples, which had the smallest pectin concentration, had the smallest particles size. Thus, it appears that the smallest content of pectin leads to smallest particle size at higher temperatures.

Table 2
The specific surface areas of the samples

Sample	Temperature (°C)	BET singlepoint (m^2/g)	BET multipoint (m^2/g)	Standard deviation (m^2/g)
A		83.84	87.14	±0.468
B	500	86.83	89.99	±0.395
C		79.63	82.61	±0.448
A		41.75	43.31	±0.145
B	700	38.08	39.28	±0.094
C		33.73	34.91	±0.063
A		20.28	21.04	±0.052
B	900	18.22	18.84	±0.056
C		18.89	19.52	±0.083
A		10.09	10.71	±0.046
B	1000	6.86	7.33	±0.041
C		8.20	8.67	±0.032

The effect is only slight, and we are not yet sure of the precise reason for this. This effect, and the mechanism behind, requires further investigation.

Note that there are reasons why the particle size from BET analyses may be slightly high, such as the formation of solid bridges between the particles, and non-sphericity of the particles.

The sucrose and pectin polymeric matrix serves as an efficient internal fuel to decompose and burn out the precursor into a refined metal oxide powder at low temperature. Thus, the surface area of the final powders depend on the total effects of both generated gas and heat. When the ratio of sucrose to metal ions has an optimum value powders with high surface area will be produced.

4.4. X-ray analysis

X-ray diffraction (XRD) was carried out with Cu Kα radiation on a Brucker D-8 Advance X-ray diffractometer. The unit cell parameter accuracy is $\pm 10^{-3}$ Å. The intensities were measured from 20 to 100° with a step size of 0.02° and a counting rate of 3 s per scanning step. The X-ray diffraction spectra showed that the obtained nanoparticles at temperatures between 500 and 1000 °C are stabilized in the cubic crystal form matching reference pattern no. 30-1468 according to the International Center for Diffraction Data (ICDD). The pattern corresponds to yttrium zirconium oxide—$Y0.15Zr0.85O1.93–92ZrO_28Y_2O_3$. The presence of other phases such as monoclinic or tetragonal zirconia or of free Y_2O_3 was not observed. Thus, a homogeneous solid solution of Y_2O_3 with ZrO_2 was formed which existed in a cubic crystal structure. It can be observed that for the sample calcined at 500 °C the peaks are much broader (see Fig. 5) which indicates that the crystallites are smaller. Also, the noise of the spectrum is much more intense, probably due to the smaller crystallite size. Increasing the calcination temperature to 1000 °C, the peaks become progressively more narrow and also the noise is reduced, indicating that the crystallite size is increased.

The Scherrer formula (Eq. (4)) was applied to the first four peaks of the obtained XRD spectrum in order to determine the

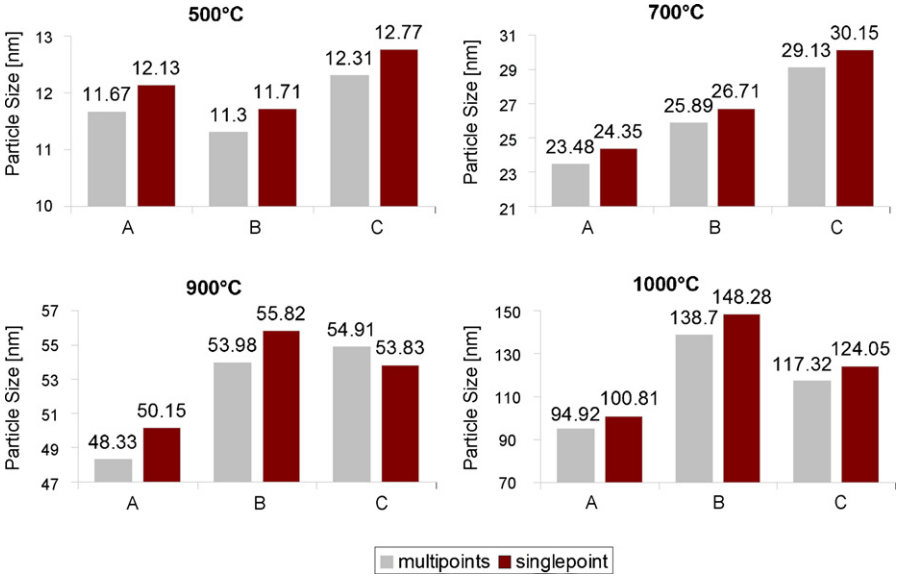

Fig. 4. The mean particle size of A, B and C samples at 500, 700, 900 and 1000 °C.

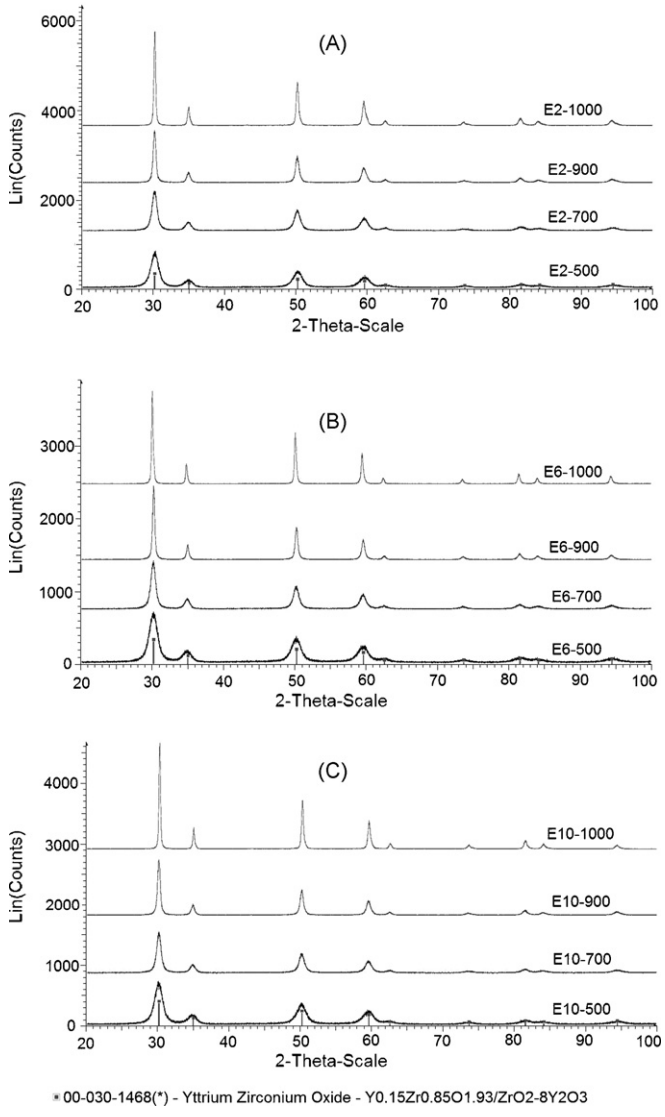

Fig. 5. The X-ray diffraction spectra size of A, B and C samples at 500, 700, 900 and 1000 °C.

crystallite size of the powder:

$$D = \frac{k\lambda}{B\cos\theta} \quad (4)$$

where k is a constant, here taken as unity, λ the wavelength of Cu Kα1, taken as 0.15406 nm, B the width of the peak (FWMH) in radians, and 2θ is the angle of the mode of the peak. The full width at half maximum (FWHM) and the 2θ values determined from the XRD spectrum together with the calculated crystallite size of the B samples calcined at 500 and 1000 °C temperatures are shown in Table 3. We show these values to demonstrate that the FWHM and the estimates of crystallite size are consistent between the peaks although they have very different heights. All the data show the FWHM to decrease with increasing temperature indicating an increase in the particle size with increasing temperature.

In Fig. 6, the crystallite size for the A, B and C samples are shown at each temperature in the studied interval. In agreement with the BET data, the XRD data show that the B composition presents the smallest crystallite sizes at low temperatures (6.69 nm), while at high temperatures the A samples have the smallest crystallite sizes (26.72 nm).

Table 3
The XRD data of the B samples at 500 and 1000 °C

Sample	Temperature (°C)	Peak	FWHM (°)	2θ Obs. Max. (°)	Crystallite size (nm)
B	500	1st	1.354	30.121	6.751
		2nd	1.380	34.819	6.703
		3rd	1.514	50.180	6.438
		4th	1.479	59.275	6.866
B	1000	1st	0.256	29.930	35.691
		2nd	0.269	34.724	34.380
		3rd	0.288	50.012	33.819
		4th	0.339	59.468	29.986

4.5. Transmission electron microscopy

The JEOL-JEM-1011 transmission microscope was used to examine the morphology of the all samples (see Fig. 7). The obtained nanoparticles have shown relatively uniform and rounded shapes with a narrow size distribution. The samples were dispersed in water under stirring and one drop taken from the solution was deposited on a copper grid. Previous to this, the grids had undergone a carbon deposition process under vacuum followed by a glow discharge. According to the measurements performed on the TEM images the mean particle size of the samples were calculated and values such as 10.3 nm for A sample, 9.1 nm for B sample and 8.3 nm for C sample at 500 °C were found. At 1000 °C, the mean particle size of the samples were found to be 58.7 nm for A sample, 36.9 nm for B sample and 55.13 nm for C samples, respectively. As the TEM data have shown, the calcination temperature influences the mean particle size of the samples and they varied between 8.3 and 58.7 nm. It was apparent that obtained nanoparticles of the samples calcined at 500, 700 and 1000 °C were well dispersed, very uniform and only slight agglomeration occurred at high temperature. This indicated the calcination process of yttria-stabilized zirconia nanoparticles prepared by this sol–gel method into larger particles or agglomerates could be effectively slowed

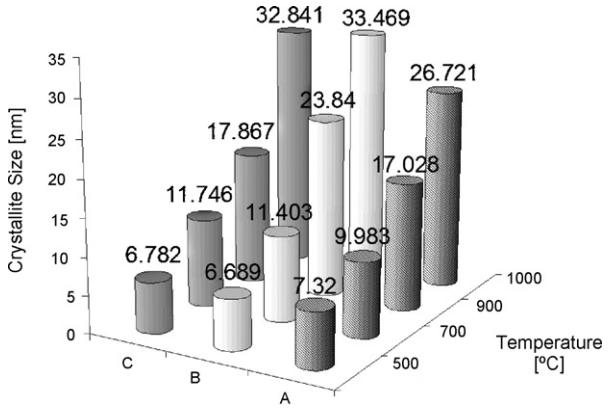

Fig. 6. The crystallite size of the samples determined by XRD.

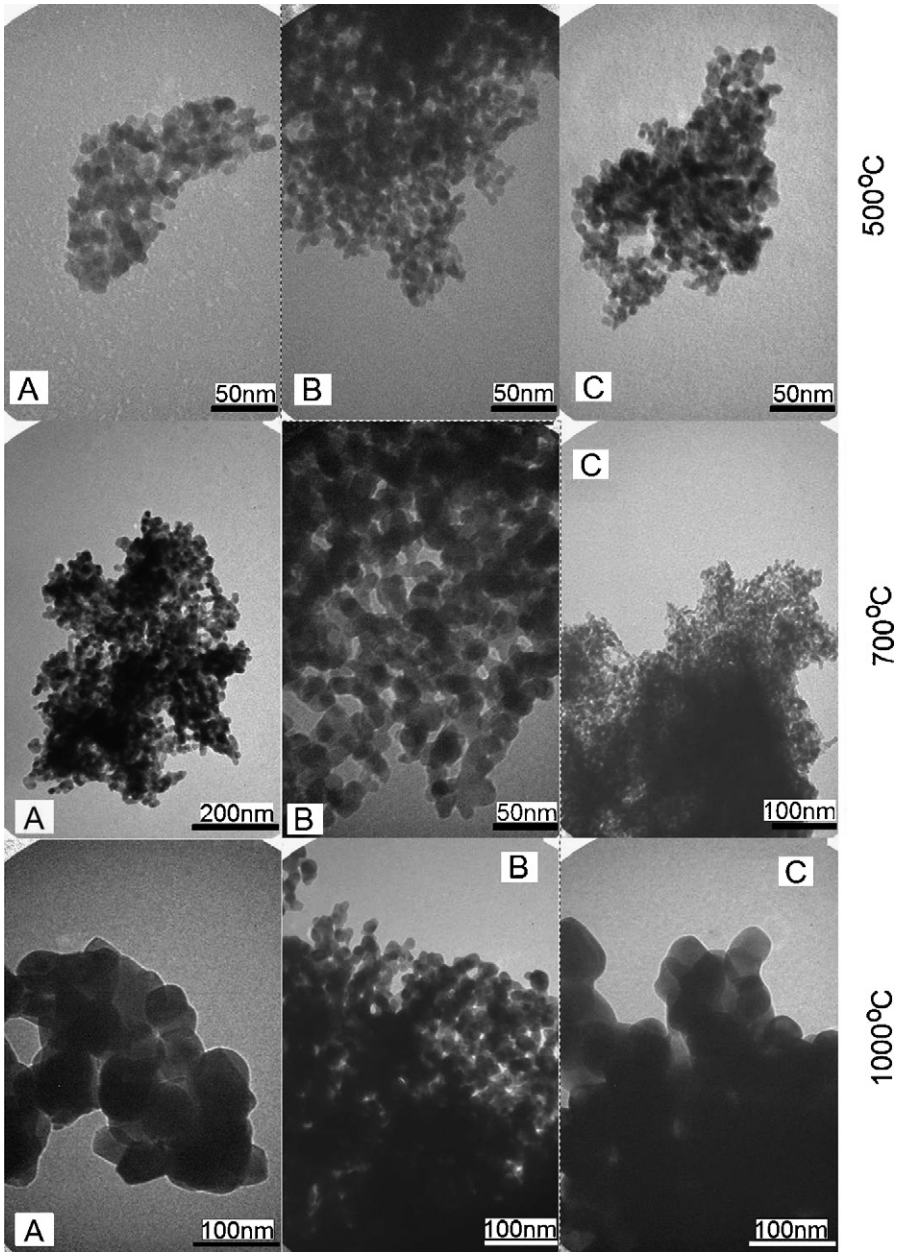

Fig. 7. The TEM images of the samples at 500, 700 and 1000 °C.

down through the addition of sucrose:pectin ratio even at higher temperatures.

5. Concluding remarks

The influence of the process parameters on the properties of nanoparticles produced with a new sol–gel process using sucrose and pectin in place of conventional organic precursors has been investigated. The study has led to the following conclusions:

- The polymeric matrix of sucrose and pectin has two important functions as
  (i) a solid dispersoid and
  (ii) a solid fuel.

  Sucrose acts as a chelating agent and template material. Homogeneous distribution of metal ions and large amount of generated gas during calcinations reduced agglomeration of particles and gave rise to very high surface area in the final powders.
- The XRD data indicate cubic ZrO_2 already for a calcination temperature 500 °C, confirming that the solid solution process was completed in all cases. Other crystalline phases were not observed. The noise in the spectra reduced with increasing calcination temperature. The crystallite size determined by the Scherrer formula varied between 6–7 nm at 500 °C and 26–33 nm at 1000 °C.
- The singlepoint and multipoint BET analyses (Fig. 4) and XRD/Scherrer formula analyses (Fig. 6) agree in showing the highest particle size/crystallite size for sample B and the

lowest for sample A. The two analysis method also agree well in terms of trend for the other temperatures.

- The absolute particle size according to the BET is quite a lot higher than the crystallite size from the XRD. Here the "final word" is the TEM, which shows particle sizes intermediate between the two: 8.3–10.3 nm at 500 °C and 37–58 nm at 1000 °C. These values are close to the crystallite sizes, indicating that one particle generally consists of one crystal. TEM does not give a good estimate for the average particle size.
- In spite of the differences found, it can be concluded that the process is quite tolerant to the ratio of pectin to glucose. The effect of the calcination temperature is more crucial, and this can be used to tailor the particle properties.

Acknowledgments

This work was funded by the NFR (Norwegian Research Council) and PROTOTECH A.S., Bergen, Norway made laboratory facilities available. Also, the authors are grateful to Senioringeniør Egil Erichsen (Laboratory for Electron Microscopy) and to Prof. Karl Wilhelm Törnroos (Department of Chemistry) University of Bergen, Norway for help and useful discussions.

References

[1] V. Esposito, D.Z. de Florio, F.C. Fonseca, E.N.S. Muccillo, R. Muccillo, E. Traversa, Electrical properties of YSZ/NiO composites prepared by a liquid mixture technique, J. Eur. Ceram. Soc. 25 (2005) 2637–2641.

[2] Y. Sunagawa, K. Yamamoto, A. Muramatsu, Improvement in SOFC anode performance by finely-structured Ni/YSZ cermet prepared via heterocoagulation, J. Phys. Chem. B 25 (2006) 6224–6228.

[3] B. Wei, Z. Lu, X. Huanga, M. Liu, K. Chena, W. Sua, Enhanced performance of a single-chamber solid oxide fuel cell with an SDC-impregnated cathode, J. Phys. Chem. B 167 (2007) 58–63.

[4] E. Djurado, F. Boulc'h, A.P.Y. Frolov, N. van Landschoot, J. Schoonman, Cold isostatic and explosive isodynamic compaction, Solid State Ionics 154 (Part B) (2002) 375–380.

[5] R. Habermann, T. Fukui, Solid oxide fuel cells by a new generation of powder processor, CFI-ceramic forum international 84 (2007) E14–E20.

[6] T. Hernandez, C. Bautista, P. Martin, Synthesis and thermal evolution of Mn-doped alumina nanoparticles by homogeneous precipitation with urea, Mater. Chem. Phys. 92 (2005) 366–372.

[7] E.E. Sileoa, R. Rotelo, S. Jacobo, Nickel zinc ferrites prepared by the citrate precursor method, Phys. B 320 (2005) 257–260.

[8] Z. Xiu, M. Lu, S. Liu, G. Zhou, B. Su, H. Zhang, Barium hydroxyapatite nanoparticles synthesized by citric acid sol–gel combustion method, Mater. Res. Bull. 40 (2005) 1617–1622.

[9] C.H. Lu, W.T. Hsu, J. Dhanaraj, R. Jagannathan, Sol–gel pyrolysis and photoluminescent characteristics of europium–ion doped yttrium aluminum garnet nanophosphors, J. Eur. Ceram. Soc. 24 (2004) 3723–3729.

[10] D.H. Chen, X.R. He, Synthesis of nickel ferrite nanoparticles by sol–gel method, Mater. Res. Bull. 36 (2001) 1369–1377.

[11] J. Yang, J. Liang, Q. Dong, Q. Guan, J. Chen, Z. Guo, Synthesis of YSZ nanocrystalline particles via nitrate–citrate combustion route using diester phosphate (PE) as dispersant, Mater. Lett. 57 (2003) 2792–2797.

[12] T. Meron, Y. Rosenberg, Y. Lereah, G. Markovich, Synthesis and assembly of high-quality cobalt ferrite nanocrystals prepared by a modified sol–gel technique, J. Magn. Magn. Mater. 292 (2005) 11–16.

[13] F. Snijkers, A. de Wilde, S. Mullens, J. Luyten, Aqueous tape casting of yttria stabilised zirconia using natural product binder, J. Eur. Ceram. Soc. 24 (2004) 1107–1110.

[14] C. Suciu, L. Gagea, A.C. Hoffmann, M. Mocean, Sol–gel production of ZrO_2 and 8YSZ with a new organic precursor, Chem. Eng. Sci. 61 (2006) 7831–7835.

[15] Y. Wu, A. Bandyopadhyay, S. Bose, Processing of alumina and zirconia nanopowders and compacts, Mater. Sci. Eng. A 380 (2004) 349–355.

[16] J. Ray, R.K. Pati, P. Pramanik, Chemical synthesis and structural characterization of nanocrystalline powders of pure zirconia and yttria stabilized zirconia (YSZ), J. Eur. Ceram. Soc. 20 (2000) 1289–1295.

[17] J.C. Ray, P. Pramanik, S. Ram, Formation of Cr_3 stabilized ZrO_2 nanocrystal in a single cubic metastable phase by a novel chemical route with a sucrose polyvinyl alcohol polymer matrix, Mater. Lett. 48 (2001) 281–291.

[18] P. Pramanik, A novel chemical route for the preparation of nanosized oxides, phosphates, vanadates, molybdates and tungstates using polymer precursors, Bull. Mater. Sci. 22 (1999) 335–339.

[19] W.G.T. Willats, J.P. Knox, J.D. Mikkelsen, Pectin: new insights into an old polymer are starting to gels, Trends Food Sci. Tech. 17 (2006) 97–104.